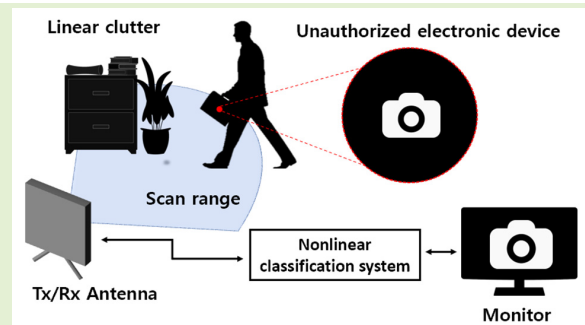


# Nonlinear Radar-Based Classification System for Electronic Devices in Cluttered Close-Range Scenarios

Wonryeol Lee<sup>1</sup>, Graduate Student Member, IEEE, Sooyoung Oh<sup>1</sup>, Graduate Student Member, IEEE, and Sun K. Hong<sup>1</sup>, Senior Member, IEEE

**Abstract**—This article proposes a system for detecting and classifying realistic electronic devices in the presence of linear clutter objects based on a frequency-modulated continuous-wave (FMCW) nonlinear radar. For classification, the proposed system utilizes statistical features of the time-segmented baseband signal envelope of the second harmonic responses from targets, which contain nonlinear coefficients of targets, and a support vector machine (SVM) is used as the classifier. The system is validated using an experimental apparatus in an anechoic chamber, and a minimum allowable signal-to-noise ratio (SNR) is set to ensure accurate target classification in the presence of a linear clutter object. The transmit frequency band of the FMCW nonlinear radar used for the experiment is 3.0–3.2 GHz, and the receive frequency band is 6–6.4 GHz, which is the second harmonic of the transmit band. The experimental results show that the proposed system can detect and classify targets with a detection rate of 85.5% and classification accuracy of 89.2%. The proposed system has the potential to provide an effective solution for detecting and classifying unauthorized electronic devices in various scenarios.

**Index Terms**—Frequency-modulated continuous-wave (FMCW), machine learning, nonlinear radar, support vector machine (SVM), target classification.



## I. INTRODUCTION

THE continuous increase in semiconductor performance and the development of engineering technology have led to a surge in the use of small electronic devices, making it easy for anyone to possess them. However, the proliferation of these devices has also led to an increase in their malicious use. As a result, there is a growing need for technologies capable of detecting and classifying unauthorized and hidden electronic devices at a stand-off distance. Existing linear radar has a limitation in detecting a relatively small target in the presence of linear clutter. To overcome such difficulties, research on nonlinear radar that detects harmonics or

intermodulations, which are nonlinear responses excited only from electronic components, has been widely conducted [1], [2], [3], [4], [5], [6], [7]. However, target classification beyond detection requires a complex interpretation of received signals. To overcome this, recent research has enabled target identification using machine learning by extracting features based on the target radar cross section (RCS) [8], [9], [10] and Doppler characteristics [11], [12], [13], [14], [15], [16], [17], [18], [19] in linear radars. Recently, research has been conducted on target recognition based on the characteristics of nonlinear target responses through simulations [20], [21], [22], [23]. In our previous work, the feasibility of nonlinear target classification using support vector machines (SVMs) for a frequency-modulated continuous-wave (FMCW)-based nonlinear radar system was demonstrated, where statistical characteristics from the second harmonics excited from several realistic nonlinear targets are used as features [24]. However, this study was conducted in an environment in which only a target of interest was present, and the algorithm was not tested with nonlinear targets in an environment where a linear object coexists. In addition, in [24], target features were extracted from the spectrum of the nonlinear responses directly sampled at RF. However, in a realistic system, to apply nonlinear target

Received 29 October 2024; accepted 13 November 2024. Date of publication 25 November 2024; date of current version 2 January 2025. This work was supported in part by the Institute of Information and Communications Technology Planning and Evaluation (IITP) through the Korean Government [Ministry of Science and Information and Communication Technology (MSIT)] (Efficient Design of RF Components and Systems Based on Artificial Intelligence, 100%) under Grant RS-2024-00393808. The associate editor coordinating the review of this article and approving it for publication was Prof. Takuya Sakamoto. (Corresponding author: Sun K. Hong.)

The authors are with the School of Electronic Engineering, Soongsil University, Seoul 06978, South Korea (e-mail: dldnjsuf1@soongsil.ac.kr; callme987@soongsil.ac.kr; shong215@ssu.ac.kr).

Digital Object Identifier 10.1109/JSEN.2024.3502209

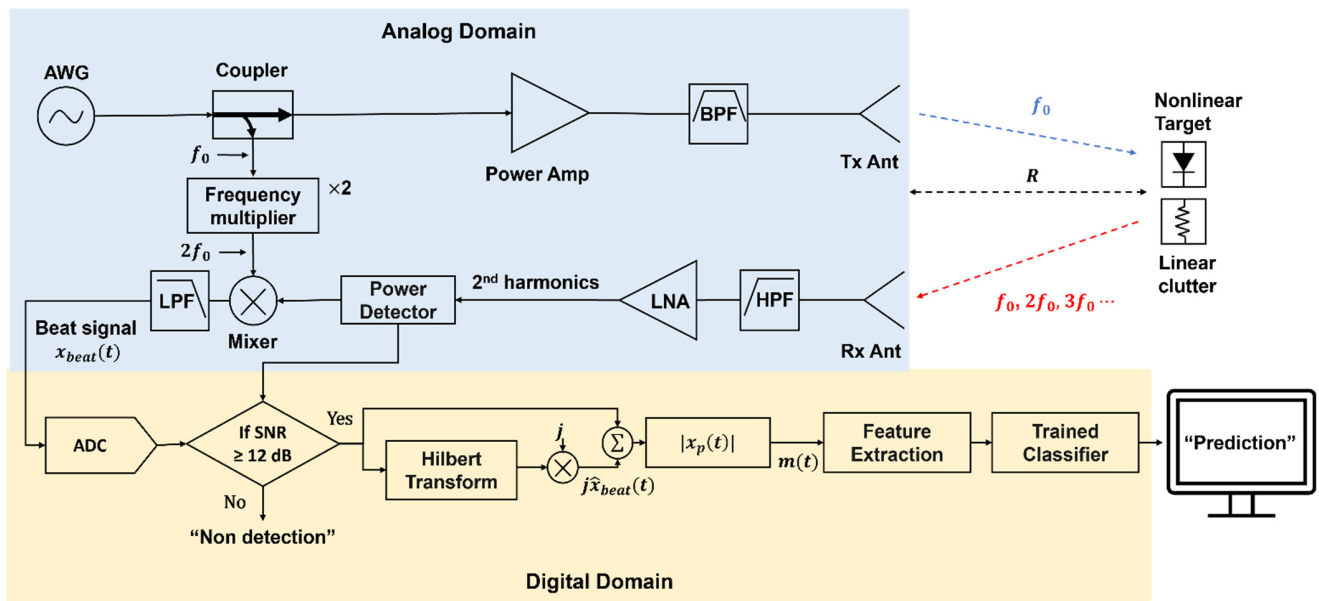


Fig. 1. Block diagram of the proposed notional system used in this article.

classification based on frequency-specific nonlinear responses, as demonstrated in our previous study, it is necessary to conduct classification using the beat signal of the baseband.

In scenarios where linear clutter objects coexist, the decrease in signal-to-noise ratio (SNR) results in decreased classification accuracy [23]. Additionally, multipath effects can cause false alarms, seriously affecting the performance of the nonlinear target detection [25], [26]. Therefore, to ensure accurate target classification, it is necessary to set a minimum allowable SNR [2], [23].

In this article, we use an experimental apparatus representing an FMCW-based nonlinear radar to measure the second harmonic responses of several realistic electronic targets. The beat signals, which are extracted through signal processing, undergo target classification via SVM through a segment-based statistical feature extraction process while setting a minimum allowable SNR to validate successful detection. The proposed concept, along with the proposed notional radar system, has the potential to provide an effective solution for detecting and classifying electronic devices as depicted in Fig. 1. Fig. 1 provides an overview of the system aiming to detect and classify the nonlinear target in an environment where the linear clutter object is present nearby.

The organization of this article is as follows. In Section II, a theoretical analysis of the beat signals of the target harmonic responses is conducted to demonstrate the potential for using their characteristics in target classification. In Section III, the feature extraction method used to experimentally demonstrate the proposed system, and the experimental setup are explained. In Section IV, the detection method based on SNR, the process of SVM training, and the analysis of the results are presented. Finally, Section V concludes this article with a summary.

## II. HARMONIC RESPONSE ANALYSIS IN BEAT SIGNAL

Signals incident at a nonlinear target generate harmonics as a result of nonlinear interaction. In the time domain, the

harmonic responses for such signals can be expressed using a power series model [1], [28] as

$$x_r(t) = \sum_{n=1}^{\infty} [a_n(x(t))^n] \quad (1)$$

where  $x_r(t)$  is the reflected signal from the nonlinear target, and  $x(t)$  is the incident signal at the target. The harmonic coefficient  $a_n$  can vary depending on the frequency of  $x(t)$  since the nonlinear excitation at the target may be frequency-dependent.

For an FMCW radar, the transmit signal can be expressed as

$$x(t) = \cos\left(\omega_0 t + \frac{\pi BW}{T_m} t^2\right) \quad (2)$$

where  $\omega_0$  is the starting frequency,  $BW$  is the chirp bandwidth, and  $T_m$  is the chirp duration. Typically for a nonlinear target, the level of generated harmonics decreases as the order  $n$  increases and consequently the value of the higher-order  $a_n$  becomes significantly small. Therefore, by substituting  $x(t)$  of (2) into (1) and expanding up to the fourth order where the second harmonic component exists, the derived equation for the received signal of the second harmonic response from the target can be represented as

$$x_{r,2}(t) \approx \left[ \frac{a_2(\omega(t)) + a_4(\omega(t))}{2} \right] \cdot \cos\left(2\omega_0(t - \Delta t) + \frac{2\pi BW}{T_m}(t - \Delta t)^2\right) \quad (3)$$

where  $\omega(t) = \omega_0 + (\pi BW/T_m)(t - \Delta t/2)$ , which indicates that  $a_2$  and  $a_4$  are functions of time, since  $\omega(t)$  is a function of time. A properly received  $x_{r,2}(t)$  then can be down-converted by mixing with frequency-doubled  $x(t)$ , and low-pass-filtered

to obtain the beat signal expressed as follows:

$$\begin{aligned} x_{\text{beat}}(t) &= \left[ x_{r,2}(t) \cdot \cos\left(2\omega_0 t + \frac{2\pi BW}{T_m} t^2\right) \right] * h_{\text{LPF}}(t) \\ &= \left\{ \frac{a_2(\omega(t)) + a_4(\omega(t))}{4} \right\} \\ &\quad \times \left\{ \cos\left[\Delta t \left(2\omega_0 + \frac{2\pi BW}{T_m} (2t - \Delta t)\right)\right] \right\} \end{aligned} \quad (4)$$

where  $h_{\text{LPF}}(t)$  is the impulse response of the low pass filter,  $\Delta t = 2R_0/c$  is the time delay associated with the target distance  $R_0$ , and  $c$  is the speed of electromagnetic waves. The process of extracting the target's distance in a nonlinear FMCW radar system is explained in detail in [2]. In (4), the amplitude term of the beat signal contains nonlinear coefficients  $a_2$  and  $a_4$ . As mentioned above, these nonlinear coefficients may vary with  $\omega(t)$ , suggesting that for FMCW-based nonlinear radars, the nonlinear coefficients of the target response could vary over time. Therefore, the amplitude of  $x_{\text{beat}}(t)$  also varies with time. Moreover, under the assumption that the nonlinear coefficients do not have periodicity over time within the chirp duration, applying the Hilbert transform enables the extraction of the signal envelope  $m(t)$  of  $x_{\text{beat}}(t)$  as follows:

$$\begin{aligned} x_p(t) &= x_{\text{beat}}(t) + j\hat{x}_{\text{beat}}(t) \\ &= \left\{ \frac{a_2(\omega(t)) + a_4(\omega(t))}{4} \right\} e^{j2\omega_0\Delta t + j\frac{2\pi BW}{T_m}(2\Delta t - \Delta t^2)} \end{aligned} \quad (5)$$

$$m(t) = |x_p(t)| = \left| \frac{a_2(\omega(t)) + a_4(\omega(t))}{4} \right|. \quad (6)$$

From (5) and (6), it can be seen that the beat signal as a result of down-conversion with the frequency-doubled local oscillator signal contains information regarding the nonlinear response characteristics of the nonlinear targets, which can be used for the feature extraction and the target classification.

### III. FEATURES AND SYSTEM CONSTRUCTOR

In machine learning, feature extraction is the most influential factor in determining classification performance. Namely, the better the features that represent the characteristics of each target, the better the classifier performance. In target classification based on linear FMCW radars, there are instances where various statistical parameters have been successfully used for the classification [19]. Moreover, statistical parameters can also be utilized in identifying nonlinear targets through their nonlinear coefficients [20], [21], [22], [23].

#### A. Feature Extraction

An example of the baseband envelope  $m(t)$  of the nonlinear response from the nonlinear target is shown in Fig. 2, which exhibits a time-dependent behavior due to the time-varying frequency modulation. Here,  $m(t)$  undergoes the process of segmentation to extract statistical features [24]. Subsequently,  $m(t)$  is divided into  $p$  number of segments, and statistical parameters such as mean ( $\mu$ ), variance ( $\nu$ ), and variance coefficient ( $c$ ) are extracted using the following equations

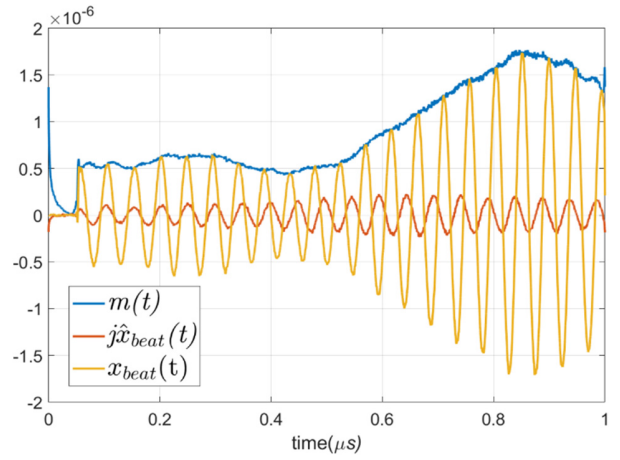


Fig. 2. Beat signal incorporated into the nonlinear response of the sample.

for each segment to capture the magnitude and variability characteristics of the nonlinear response:

$$\mu_{i,k} = \frac{1}{N} \sum_{n=1}^N m_{i,k}(n) \quad (7)$$

$$\nu_{i,k} = \frac{1}{N-1} \{m_{i,k}(n) - \mu_{i,k}\}^2 \quad (8)$$

and

$$c_{i,k} = \frac{\sqrt{\nu_{i,k}}}{\mu_{i,k}} \quad (9)$$

where  $k$  is the segment index,  $i$  is the measurement data index, and  $N$  is the number of samples in a segment. In Fig. 3, the statistical parameter values for each segment of one of the nonlinear targets used (i.e., dash camera) are shown. These statistical parameters form a set  $\mathbf{S}_i$  as follows:

$$\mathbf{S}_i = \{\mu_{i,k}, \nu_{i,k}, c_{i,k} | 1 \leq k \leq p\}. \quad (10)$$

In (10), it can be observed that the size of  $\mathbf{S}_i$  varies depending on  $p$ . As  $p$  increases, the growth in size  $\mathbf{S}_i$  may result in an extended training time and the potential for overfitting. To determine a reasonable value of  $p$ , the hyperparameters of the SVM are fixed, and the performance of the classifier based on the number of segments is examined, as shown in Fig. 4. As the number of segments increases, the training accuracy improves. However, it is worth noting that when  $p$  reaches 100, the cross-validation accuracy begins to converge. An excessive increase in the number of segments leads to an increase in the feature count used for the SVM training, resulting in an increased computational cost and the curse of dimensionality [29]. Consequently, considering these outcomes, the optimal value of  $p$  is set to 100.

#### B. Measurement Setup

To experimentally validate the proposed concept, a measurement setup is configured as illustrated in Fig. 5. The transmit-end consists of a Tektronix AWG7102 arbitrary waveform generator to generate the transmit FMCW waveforms over the bandwidth of 3–3.2 GHz with a chirp duration

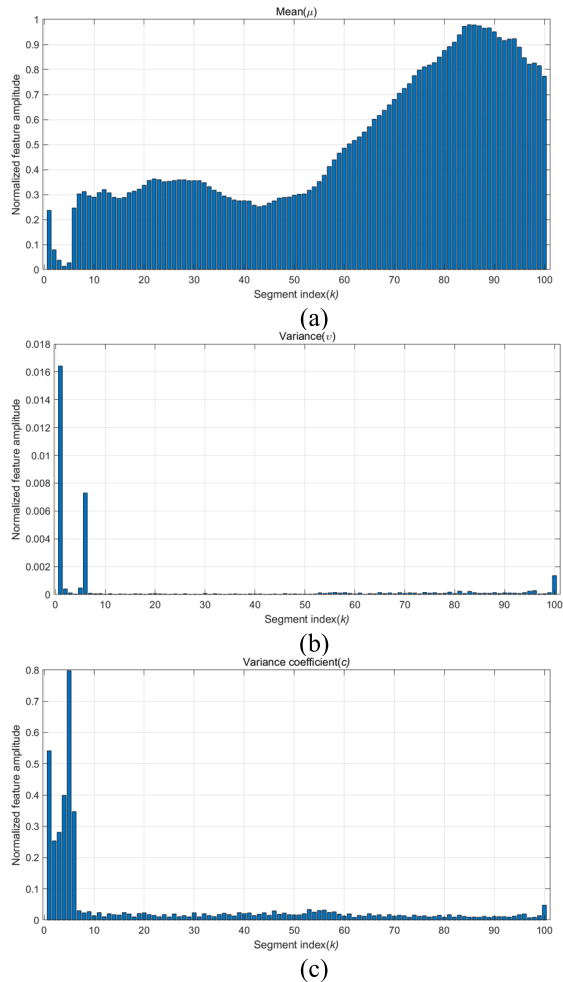


Fig. 3. Example baseband envelope of (a) mean ( $\mu$ ), (b) variance ( $\nu$ ), and (c) variance coefficient ( $c$ ).

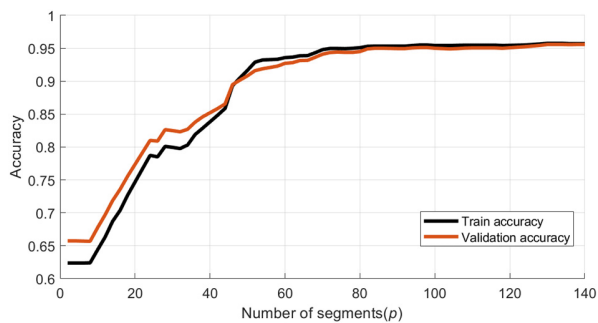


Fig. 4. Train and validation accuracy based on the number of segments.

of  $1 \mu\text{s}$ . The waveforms are then amplified to 41.2 dBm (13.18 W) using an Ophir 5183 RF power amplifier. The second harmonics generated by the power amplifier become a performance degradation factor for target detection and classification through linear reflection and antenna coupling. Therefore, a Wainwright WLJ5 low pass filter is included along the transmit path after the power amplifier to suppress self-generated harmonics. The transmit waveforms are radiated through a 3160-09 standard gain horn antenna with a gain of 17.6 dBi. The receive-end is composed of a VT58SGAH20NK standard gain horn antenna with a gain of 20 dBi, followed by

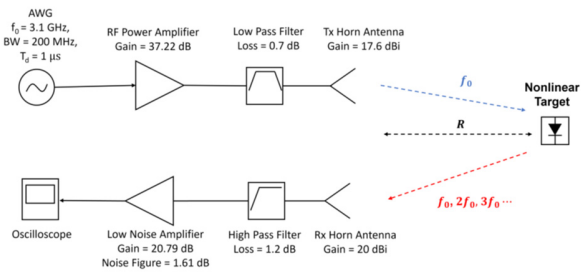


Fig. 5. Block diagram of the measurement setup.

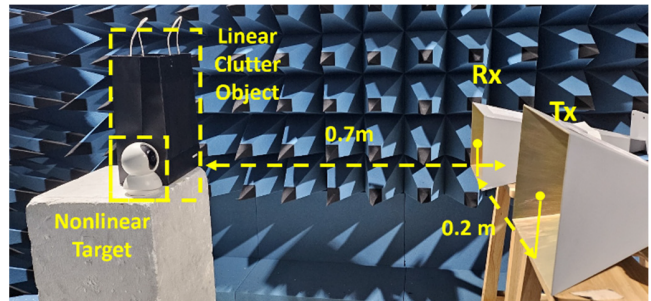


Fig. 6. Photograph of the experiment setup.

a VBFZ-6240-S+ C-bandpass filter to suppress the fundamental band. A ZX60-83LN12+ low noise amplifier with a gain of 20.79 dB is used to boost the received harmonic responses from the target before acquisition via a TDS6154C fast-sampling oscilloscope. The proposed notional system depicted in Fig. 1 involves the down-conversion of  $x_{r,2}(t)$  into  $x_{\text{beat}}(t)$  in the analog domain using a mixer and filter, followed by an analog-to-digital converter (ADC). However, it is to be noted that in our experiment,  $x_{r,2}(t)$  is directly sampled through the oscilloscope and the down-conversion is done in the signal processing to obtain  $x_{\text{beat}}(t)$ . Such an approach enables us to employ a simplified experimental apparatus for the validation of the proposed concept. As shown in Fig. 6, the transmit/receive antennas and targets are placed in an anechoic chamber. The distance between the antennas and the target was set to 0.7 m to detect the weak nonlinear responses of commercial electronic devices. Fig. 7 shows the nonlinear targets used in our experiment, including a dash camera, web camera, radio, remote switch, and drone, while Fig. 8 shows three linear clutter objects (metal tumbler, paper bag, brick) which are placed alongside the targets during the measurement.

## IV. TRAINING AND RESULT

### A. Training Classifier With Nonlinear Targets Only

To train the SVM classifier, approximately 1006 harmonic response measurements of each target (about 200 per target) are performed in an environment where only nonlinear targets exist. The baseband signals  $x_{\text{beat}}(t)$  are processed to obtain  $m(t)$  for feature extraction mentioned in Section II.

The 1006 sets of  $\mathbf{S}_i$  are divided into training data and verification data for the SVM classifier learning with a ratio of 7:3, respectively. The learning results of the SVM classifier are shown in Table I. The training accuracy of 96.6%,

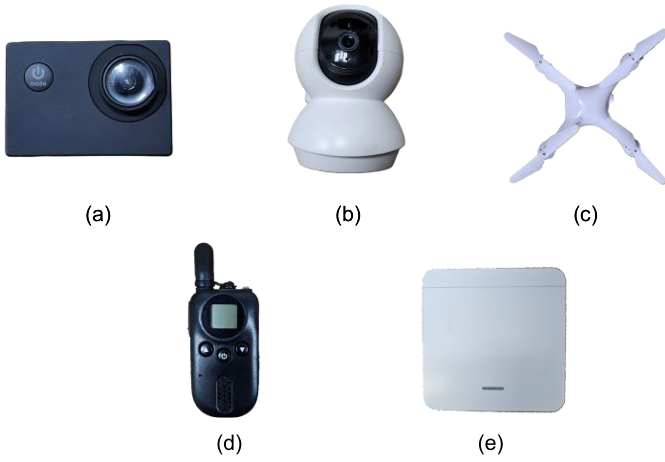


Fig. 7. Nonlinear targets (a) dash camera ( $5 \times 7 \text{ cm}^2$ ), (b) web camera ( $10 \times 15 \text{ cm}^2$ ), (c) drone ( $25 \times 25 \text{ cm}^2$ ), (d) radio ( $3.5 \times 9 \text{ cm}^2$ ), and (e) remote switch ( $8 \times 8 \text{ cm}^2$ ).

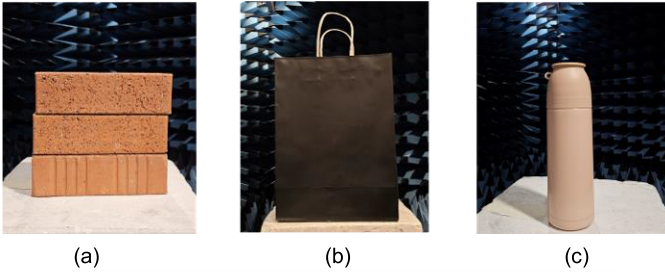


Fig. 8. Linear clutter objects used for measurement. (a) Paper bag ( $30 \times 30 \text{ cm}^2$ ). (b) Bricks ( $27 \times 25 \text{ cm}^2$ ). (c) Tumbler ( $7 \times 21 \text{ cm}^2$ ).

TABLE I  
CONFUSION MATRIX OF TRAIN DATA (UNIT: %)

Estimated class / Actual class	Dash cam	Web camera	Drone	Radio	Remote switch
Dash cam	100	0	0	0	0
Web camera	0	100	0	0	0
Drone	0	0	80	20	0
Radio	0	0	0	100	0
Remote switch	0	0	0	0	100

validation accuracy of 96.0%, and threefold cross-validation mean accuracy of 97.2% are used to classify detected targets.

### B. Prediction and Results in Cluttered Environment

The test data consists of the second harmonic responses when linear clutter objects and nonlinear targets coexist. The total number of test data is 772, consisting of about 50 combinations for each type of nonlinear target and linear clutter object. The noise data used for SNR calculation is applied to the signals with only linear clutter objects in the setup. As shown in Fig. 9, when the signal amplitude is above the minimum allowable SNR, the feature extraction method used for classification employs the statistical parameter extraction method described in Section III-A. The detection results for the test data are presented in Table II, showing an average detection rate of 85.5%. The SVM classification

TABLE II  
DETECTION RATIO OF TEST DATA (UNIT: %)

Target / Clutter	Paper Bag	Bricks	Tumbler
Dash cam	100	100	100
Web camera	100	100	100
Drone	70.6	58.8	58
Radio	74.5	23.5	100
Remote switch	100	100	100

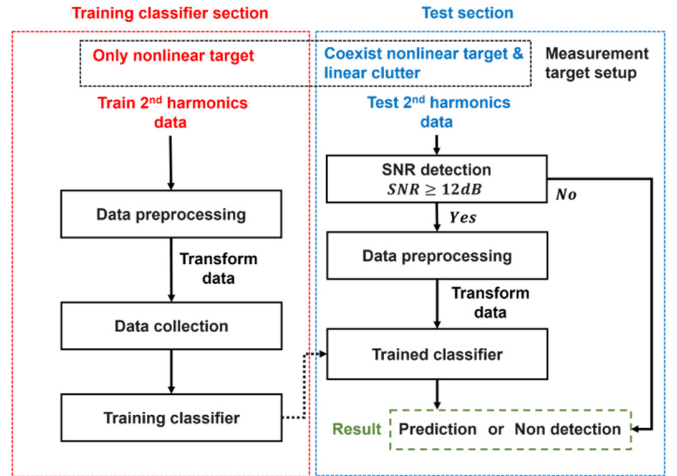


Fig. 9. Block diagram of the test data classification and detection.

results for the test data are shown in Fig. 10, with an average classification accuracy of 89.2% (bricks: 94%, paper bag: 94%, tumbler: 80.6%). The relative lower accuracy for the tumbler is attributed to the good conductive properties of the tumbler's material, causing a phase shift in the radiated harmonic signals in cluttered environments and altering the characteristics of the harmonic beat signals [25].

Additionally, the harmonic echoes originating from multipath effects can also impact the classification accuracy.

To identify the most crucial parameter in the classification process among the statistical parameters by segments in setups where a clutter object is present nearby, SVM was applied using only one parameter. Additionally, we examined the classification accuracy of the test data based on different parameter combinations, and the results are presented in Table III. Examining the results when using two parameters, in the case of a tumbler, it is observed that the accuracy is similar to when using all parameters. However, for other cases, the accuracy drops by more than 10% compared to using all parameters. This comprehensive study demonstrates the effectiveness of utilizing statistical parameter-based classification in the presence of both linear clutter and nonlinear targets. The results indicate a promising approach for enhancing the detection and classification accuracy of nonlinear targets in cluttered environments. The analysis of the impact of various parameters on classification accuracy, particularly in challenging scenarios like the tumbler case, provides valuable insights into future improvements in radar signal processing techniques.

Clutter	Paper bag					Bricks					Tumbler					
	Estimated class / Actual class	Dash cam	Web cam	Drone	Radio	Remote switch	Dash cam	Web cam	Drone	Radio	Remote switch	Dash cam	Web cam	Drone	Radio	Remote switch
Dash cam		<b>92.1 %</b>	0 %	0 %	0 %	7.9 %	<b>92.1 %</b>	0 %	0 %	0 %	7.9 %	<b>80 %</b>	0 %	0 %	0 %	20 %
Web cam	0 %	<b>100 %</b>	0 %	0 %	0 %	0 %	<b>100 %</b>	0 %	0 %	0 %	0 %	<b>100 %</b>	0 %	0 %	0 %	0 %
Drone	0 %	0 %	<b>82 %</b>	18 %	0 %	0 %	0 %	<b>82 %</b>	18 %	0 %	0 %	0 %	<b>61 %</b>	39 %	0 %	0 %
Radio	0 %	0 %	2 %	<b>98 %</b>	0 %	0 %	0 %	0 %	2 %	<b>98 %</b>	0 %	0 %	0 %	36 %	<b>62 %</b>	2 %
Remote switch	0 %	0 %	2 %	0 %	<b>98 %</b>	0 %	0 %	0 %	2 %	<b>98 %</b>	0 %	0 %	0 %	0 %	0 %	<b>100 %</b>

Fig. 10. Confusion matrix of test data with linear clutters (bold font indicates classification accuracy).

TABLE III  
AVERAGE CLASSIFICATION ACCURACY OBTAINED BY PARAMETER COMBINATION (UNIT: %)

Target / Clutter	Paper Bag	Bricks	Tumbler	Train
$\mu_{i,k}$	83.6	76.4	79.8	95.7
$\nu_{i,k}$	82.1	73.6	76.3	85.2
$c_{i,k}$	78	70.4	64	95.9
$\mu_{i,k}, \nu_{i,k}$	83.6	77.2	79.8	95.9
$\mu_{i,k}, c_{i,k}$	84.6	80.4	82	96
$\mu_{i,k}, \nu_{i,k}, c_{i,k}$	94	94	80.6	96.6

## V. CONCLUSION

This article proposes a nonlinear FMCW radar-based electronic device classification system when nonlinear targets are situated in the proximity of linear clutter objects. The theoretical expression of beat signals containing information about the nonlinear response of nonlinear targets is presented. To experimentally verify this, an SVM classifier is trained using the second harmonic responses from four nonlinear targets. The proposed system is tested in an environment where linear clutter objects and nonlinear targets coexist, achieving a detection ratio of 85.5% and classification accuracy of 89.2%. The results from this work lay the groundwork for more advanced and reliable target classification methods. However, further research is needed to investigate the detection performance based on the target angle and to identify common nonlinear characteristics within different categories of electronic devices. Such further research would allow for a wide range of practical applications in nonlinear radars for the classification of nonlinear targets.

## REFERENCES

- [1] G. J. Mazzaro, A. F. Martone, K. I. Ranney, and R. M. Narayanan, "Nonlinear radar for finding RF electronics: System design and recent advancements," *IEEE Trans. Microw. Theory Techn.*, vol. 65, no. 5, pp. 1716–1726, May 2017.
- [2] K. Cha, S. Oh, H. Hong, H. Park, and S. K. Hong, "Detection of electronic devices using FMCW nonlinear radar," *Sensors*, vol. 22, no. 16, p. 6086, Aug. 2022.
- [3] N. Nourshamsi, C. Hilton, S. Vakalis, and J. A. Nanzer, "Pulsed harmonic Doppler radar and passive RF tags for tracking the dynamic motion of held objects," *IEEE Antennas Wireless Propag. Lett.*, vol. 20, no. 5, pp. 768–772, May 2021.
- [4] K. Gallagher, R. Narayanan, G. Mazzaro, A. Martone, and K. Sherbondy, "Static and moving target imaging using harmonic radar," *Electronics*, vol. 6, no. 2, p. 30, Apr. 2017.
- [5] W. Lee, S. Oh, and S. K. Hong, "Compact dual-circularly polarized traveling-wave series-fed patch array for use as a non-linear tag antenna for bio-sensing applications," *Appl. Sci.*, vol. 13, no. 13, p. 7729, Jun. 2023.
- [6] Z.-M. Tsai et al., "A high-range-accuracy and high-sensitivity harmonic radar using pulse pseudorandom code for bee searching," *IEEE Trans. Microw. Theory Techn.*, vol. 61, no. 1, pp. 666–675, Jan. 2013.
- [7] S. Oh, H. S. Park, J. Oh, and S. K. Hong, "Circularly polarized S/C dual-band antenna for nonlinear detection," *IEEE Antennas Wireless Propag. Lett.*, vol. 21, no. 7, pp. 1467–1471, Jul. 2022.
- [8] H. Arab, I. Ghaffari, L. Chioukh, S. Tatu, and S. Dufour, "Machine learning based object classification and identification scheme using an embedded millimeter-wave radar sensor," *Sensors*, vol. 21, no. 13, p. 4291, Jun. 2021.
- [9] E. Wengrowski, M. Purri, K. Dana, and A. Huston, "Deep CNNs as a method to classify rotating objects based on monostatic RCS," *IET Radar, Sonar Navig.*, vol. 13, no. 7, pp. 1092–1100, Jul. 2019.
- [10] R. Fu, M. A. Al-Absi, K.-H. Kim, Y.-S. Lee, A. A. Al-Absi, and H.-J. Lee, "Deep learning-based drone classification using radar cross section signatures at mmWave frequencies," *IEEE Access*, vol. 9, pp. 161431–161444, 2021.
- [11] F. Fioranelli, M. Ritchie, and H. Griffiths, "Performance analysis of centroid and SVD features for personnel recognition using multistatic micro-Doppler," *IEEE Geosci. Remote Sens. Lett.*, vol. 13, no. 5, pp. 725–729, May 2016.
- [12] A. Eryildirim and I. Onaran, "Pulse Doppler radar target recognition using a two-stage SVM procedure," *IEEE Trans. Aerosp. Electron. Syst.*, vol. 47, no. 2, pp. 1450–1457, Apr. 2011.
- [13] Y. Kim, S. Ha, and J. Kwon, "Human detection using Doppler radar based on physical characteristics of targets," *IEEE Geosci. Remote Sens. Lett.*, vol. 12, no. 2, pp. 289–293, Feb. 2015.
- [14] A. Coluccia, G. Parisi, and A. Fascista, "Detection and classification of multirotor drones in radar sensor networks: A review," *Sensors*, vol. 20, no. 15, p. 4172, Jul. 2020.
- [15] G. E. Smith, K. Woodbridge, and C. J. Baker, "Radar micro-Doppler signature classification using dynamic time warping," *IEEE Trans. Aerosp. Electron. Syst.*, vol. 46, no. 3, pp. 1078–1096, Jul. 2010.
- [16] P. Kang and X. Li, "Lightweight online semisupervised learning for ultrasonic radar-based dynamic hand gesture recognition," *IEEE Sensors J.*, vol. 23, no. 3, pp. 2707–2717, Feb. 2023.
- [17] B. K. Kim, H.-S. Kang, and S.-O. Park, "Drone classification using convolutional neural networks with merged Doppler images," *IEEE Geosci. Remote Sens. Lett.*, vol. 14, no. 1, pp. 38–42, Jan. 2017.

- [18] I. Nejadgholi, H. Sadreazami, S. Rajan, and M. Bolic, "Classification of Doppler radar reflections as preprocessing for breathing rate monitoring," *IET Signal Processing*, vol. 13, no. 1, pp. 21–28, 2019.
- [19] S. Lee, B.-H. Lee, J.-E. Lee, and S.-C. Kim, "Statistical characteristic-based road structure recognition in automotive FMCW radar systems," *IEEE Trans. Intell. Transp. Syst.*, vol. 20, no. 7, pp. 2418–2429, Jul. 2019.
- [20] H. T. Hayvaci, H. Ilbegi, and I. S. Yetik, "Classification of electronic devices with power-swept signals using harmonic radar," *IEEE Trans. Aerosp. Electron. Syst.*, vol. 56, no. 3, pp. 2292–2301, Jun. 2020.
- [21] H. Taha Hayvaci, Y. Takak, and I. Samil Yetik, "A harmonic radar simulation with randomly weighted multiple ports of radiation for classification of electronic devices," *IEEE Trans. Aerosp. Electron. Syst.*, vol. 59, no. 6, pp. 9427–9437, Dec. 2023.
- [22] H. Ilbegi, H. T. Hayvaci, and I. S. Yetik, "Performance analysis of feature sets for harmonic radar to classify electronic devices," in *Proc. Int. Symp. Multidisciplinary Stud. Innov. Technol. (ISMSIT)*, Ankara, Turkey, Oct. 2022, pp. 652–655, doi: [10.1109/ISMSIT56059.2022.9932786](https://doi.org/10.1109/ISMSIT56059.2022.9932786).
- [23] H. T. Hayvaci, M. Shahi, H. Ilbegi, and I. S. Yetik, "A linear model for classification of electronic devices using harmonic radar," *IEEE Trans. Aerosp. Electron. Syst.*, vol. 57, no. 6, pp. 3614–3622, Dec. 2021.
- [24] W. R. Lee, H. Y. Hong, and S. K. Hong, "Nonlinear FMCW radar target recognition using SVM classifier," *J. Korean Inst. Electromagn. Eng. Sci.*, vol. 33, no. 7, pp. 572–575, Jul. 2022.
- [25] J. Alam, M. Khaliel, A. El-Awamry, F. Zheng, K. Solbach, and T. Kaiser, "A mathematical framework, simulation, and measurement of harmonic identification systems," *IEEE Access*, vol. 11, pp. 71811–71822, 2023.
- [26] Z. Wang, J. Yi, Z. Gong, and X. Wan, "Mechanism and characteristic of nonlinear clutter in harmonic radar with frequency-modulated waveform," *IEEE Trans. Aerosp. Electron. Syst.*, vol. 59, no. 4, pp. 4240–4249, Aug. 2023.
- [27] G. S. Woods, D. L. Maskell, and M. V. Mahoney, "A high accuracy microwave ranging system for industrial applications," *IEEE Trans. Instrum. Meas.*, vol. 42, no. 4, pp. 812–816, Aug. 1993.
- [28] S. A. Maas, *Nonlinear Microwave and RF Circuits*. Norwood, MA, USA: Artech House, 2003.
- [29] P. M. Baggenstoss, "Class-specific classifier: Avoiding the curse of dimensionality," *IEEE Aerosp. Electron. Syst. Mag.*, vol. 19, no. 1, pp. 37–52, Jan. 2004.



**Sooyoung Oh** (Graduate Student Member, IEEE) received the B.S. degree in electronic engineering from Soongsil University, Seoul, South Korea, in 2021, where he is currently pursuing the Ph.D. degree in electronic engineering.

His research interests include millimeter-wave devices, nonlinear radars, radar signal processing and antennas.



**Sun K. Hong** (Senior Member, IEEE) received the B.S. degree in electrical engineering from the University of Maryland, College Park, MD, USA, in 2005, and the M.S. and Ph.D. degrees in electrical engineering from Virginia Tech, Blacksburg, VA, USA, in 2008 and 2012, respectively.

From 2005 to 2015, he was a Research Engineer with the U.S. Naval Research Laboratory, Washington, DC, USA, where he was involved in research related to time-domain techniques in electromagnetics, nonlinear electromagnetic interaction, radars, electromagnetic scattering, high-power microwave (HPM) applications, and antennas. From 2015 to 2017, he was an Assistant Professor with the Department of Electrical and Computer Engineering, Rose-Hulman Institute of Technology, Terre Haute, IN, USA. Since 2017, he has been with Soongsil University, Seoul, South Korea, where he is currently an Associate Professor with the School of Electronic Engineering. His current research interests include the detection of nonlinear devices, radars, wavefront control techniques, wireless power transfer, EM waves in complex propagation environments, high-power electromagnetics, and antennas.



**Wonryeol Lee** (Graduate Student Member, IEEE) received the B.S. degree in electronic engineering from Soongsil University, Seoul, South Korea, in 2023, where he is currently pursuing the M.S. degree in electronic engineering.

His research interests include machine learning-based radar signal processing, antennas, and microwave devices.